Journal of Medicinal Chemistry

Article

pubs.acs.org/jmc

A Novel Semisynthetic Flavonoid 7-*O*-Galloyltaxifolin Upregulates Heme Oxygenase-1 in RAW264.7 Cells via MAPK/Nrf2 Pathway

Jiří Vrba,*[,†] Radek Gažák,[‡] Marek Kuzma,[‡] Barbora Papoušková,[§] Jan Vacek,[†] Martin Weiszenstein,[†] Vladimír Křen,[‡] and Jitka Ulrichová[†,∥]

[†]Department of Medical Chemistry and Biochemistry, Faculty of Medicine and Dentistry, Palacký University, Hněvotínská 3, Olomouc 77515, Czech Republic

[‡]Institute of Microbiology, Academy of Sciences of the Czech Republic, Vídeňská 1083, Prague 14220, Czech Republic

[§]Regional Centre of Advanced Technologies and Materials, Department of Analytical Chemistry, Faculty of Science, Palacký University, 17 listopadu 12, Olomouc 77146, Czech Republic

[∥]Institute of Molecular and Translational Medicine, Faculty of Medicine and Dentistry, Palacký University, Hněvotínská 3, Olomouc 77515, Czech Republic

Supporting Information

ABSTRACT: Quercetin and gallic acid are natural activators of the transcription factor Nrf2, which regulates the expression of many cytoprotective enzymes including heme oxygenase-1 (HO-1). We developed procedures for the synthesis of monogalloyl esters of quercetin and taxifolin (dihydroquercetin), namely, 3-*O*-galloylquercetin and 7-*O*-galloyltaxifolin, and examined their effect on the Nrf2 pathway in RAW264.7 cells. Unlike quercetin and free gallic acid, 3-*O*-galloylquercetin and natural quercetin derivatives isoquercitrin (quercetin-3-*O*-*β*-D-glucoside) and taxifolin had no effect on the expression of HO-1. In contrast, 7-*O*-galloyltaxifolin increased both mRNA and protein levels of HO-1 at concentrations of 25 *μ*M and above. The induction of HO-1 by 7-*O*-galloyltaxifolin was primarily associated with the production of reactive oxygen species and phosphorylation of mitogen-activated protein kinases (MAPKs), including p38 MAPKs and ERKs, followed by nuclear accumulation of Nrf2 and downregulation of Keap1, a negative regulator of Nrf2. We conclude that 7-*O*-galloyltaxifolin upregulates HO-1 via activation of the MAPK/Nrf2 signaling pathway.

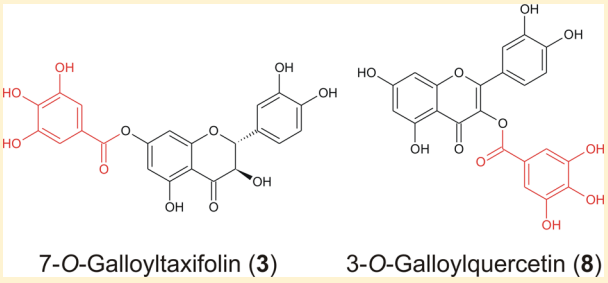

INTRODUCTION

Natural flavonoids are the largest group of plant-derived polyphenol compounds. They share a common structure consisting of two benzene rings linked through three carbons that form an oxygen-containing heterocycle. Basic flavonoid skeletons such as flavone and flavanone may carry various combinations of hydroxyl and methoxyl groups. This aside, flavonoids are predominantly found in plants as *O*-glycosides.[1] For instance, quercetin (3,5,7,3′,4′-pentahydroxyflavone; Figure 1) may occur in the form of mono-, di-, and triglycosides containing simple sugars, for example, glucose, galactose, and arabinose,[2] sugar derivatives, such as gallate and ferulate esters,[3] and various disaccharides.[2]

Dietary intake of the flavonoids present in fruits, vegetables, and beverages such as tea and wine[1] is generally considered to have beneficial health effects arising primarily from their anti-inflammatory activity. The protective action of many flavonoids may be ascribed, at least in part, to their ability to activate nuclear factor erythroid 2-related factor 2 (Nrf2).[4] Nrf2 is an important cytoprotective transcription factor responsible for both the constitutive and inducible expression of genes coding for antioxidant and phase II detoxification enzymes such as heme oxygenase-1, NAD(P)H:quinone oxidoreductase 1, catalase, thioredoxin, and glutathione *S*-transferase. The activity of Nrf2 is regulated in response to the redox imbalance caused by oxidative or electrophilic stress.[5] Under unstressed conditions, Nrf2 activity is repressed by Kelch-like ECH-associated protein 1 (Keap1), which forms a complex with Nrf2, sequesters Nrf2 in the cytoplasm, and targets Nrf2 for proteasomal degradation. In contrast, the oxidation or covalent modification of reactive cysteine residues in Keap1 produces a proteasome-dependent degradation of Keap1 followed by the stabilization and nuclear accumulation of Nrf2. In the nucleus, Nrf2 dimerizes with small Maf proteins and binds to the DNA at the antioxidant response elements to activate transcription of Nrf2 target genes.[6,7] The nuclear accumulation of Nrf2 may also be mediated via the phosphorylation of Nrf2 by various protein kinase pathways such as the p38 mitogen-activated protein kinase (p38 MAPK), extracellular signal-regulated kinase (ERK), and c-Jun N-terminal kinase (JNK) pathways. However, these protein kinase pathways regulate diverse

Received: September 17, 2012
Published: January 8, 2013

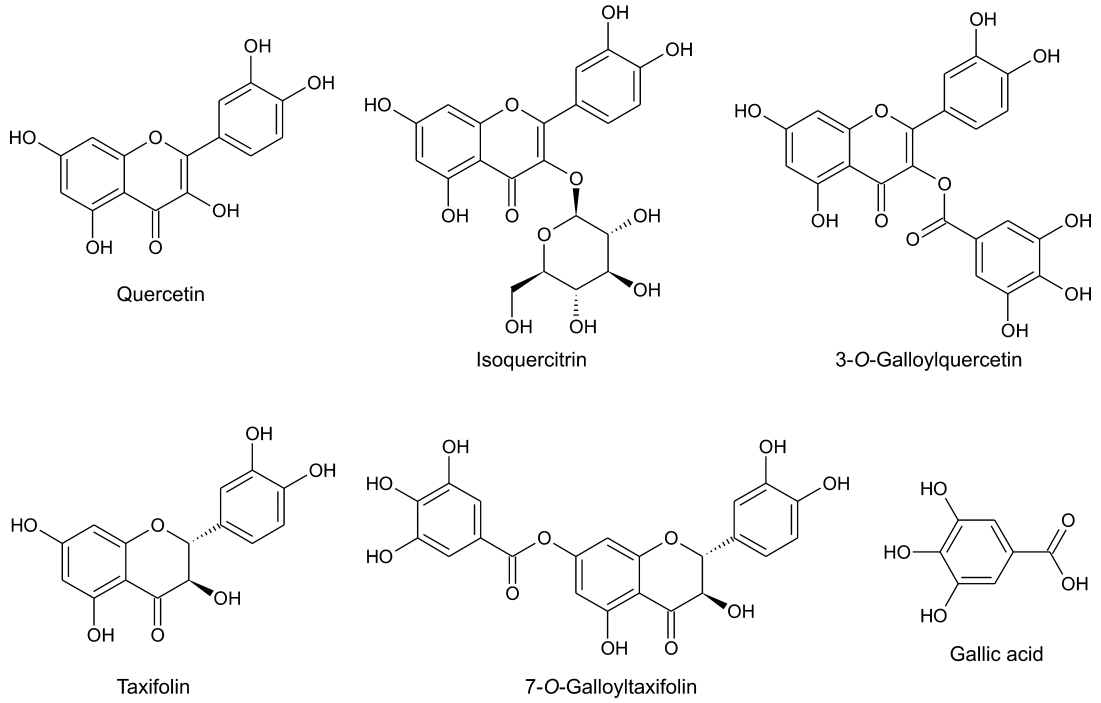

Figure 1. Chemical structures of tested phenolic compounds.

Scheme 1. Synthesis of 7-*O*-Galloyltaxifolin (3)[a]

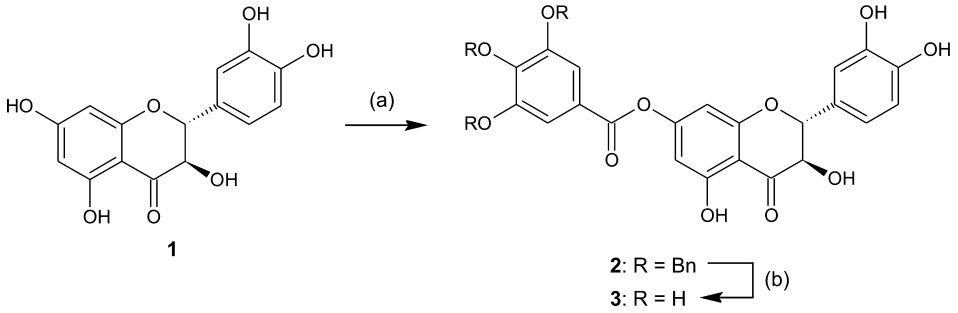

[a]Reagents and conditions: (a) 3,4,5-tri-*O*-benzylgalloyl chloride (1.5 equiv), pyridine, 0 °C, 1 h, 23%; (b) H_2–Pd/C, EtOAc, room temp, 3 h, 94%.

cellular processes, and the precise mechanisms of the phosphorylation-dependent Nrf2 activation are not fully understood.[4,7]

Classic Nrf2 activators identified among natural flavonoids are quercetin[8] and epigallocatechin-3-gallate, a flavanol carrying a galloyl ester group.[9,10] It has been shown that the ability of catechins to activate the antioxidant response element depends on the presence of a galloyl moiety in their molecules.[11] Similarly, the introduction of a galloyl moiety into the structure of the flavonolignan silybin has been found to have considerable influence on the biological activity of the resulting compound.[12] These findings inspired us to prepare galloyl esters of the prototypical flavonoid quercetin and its dihydroderivative taxifolin (dihydroquercetin; Figure 1), which both exhibit a number of biological activities.[13,14] In this study, two monogalloyl esters, 3-*O*-galloylquercetin and 7-*O*-galloyltaxifolin, were prepared, and their effect on the Nrf2 signaling pathway was examined in murine macrophage RAW264.7 cells.

CHEMISTRY

The synthesis of 7-*O*-galloyltaxifolin (**3**) was performed by direct galloylation of taxifolin (**1**) with 3,4,5-tri-*O*-benzylgalloyl chloride in pyridine (Scheme 1). The chloride of the benzyl-protected gallic acid was prepared by treating the corresponding acid with oxalyl chloride solution in CH_2Cl_2 and a catalytic amount of DMF immediately before the intended synthesis. Benzyl-containing intermediate **2** was then deprotected by catalytic hydrogenolysis with Pd on carbon, giving the final galloyl ester **3**. To achieve the galloylation of **1**, we also tested several other esterification methods, for example, the DCC/DMAP procedure, acyl chloride/Et_3N, and other methods we had previously used for the regioselective galloylation of silybin.[12] However, these methods usually gave complex mixtures of products containing only minute amounts of monogalloyl esters.

The synthesis of 3-*O*-galloylquercetin (**8**) was achieved using the strategy described in Scheme 2. The synthesis started from naturally occurring quercetin glycoside rutin (**4**). Benzylation of **4** by BnBr in DMF in the presence of Cs_2CO_3 led, after acidic hydrolysis of the intermediate glycoside, to 5,7,3′,4′-tetra-*O*-benzylquercetin (**5**). Esterification of the benzyl-protected

dx.doi.org/10.1021/jm3013344 | J. Med. Chem. 2013, 56, 856–866

Scheme 2. Synthesis of 3-*O*-Galloylquercetin (8)[a]

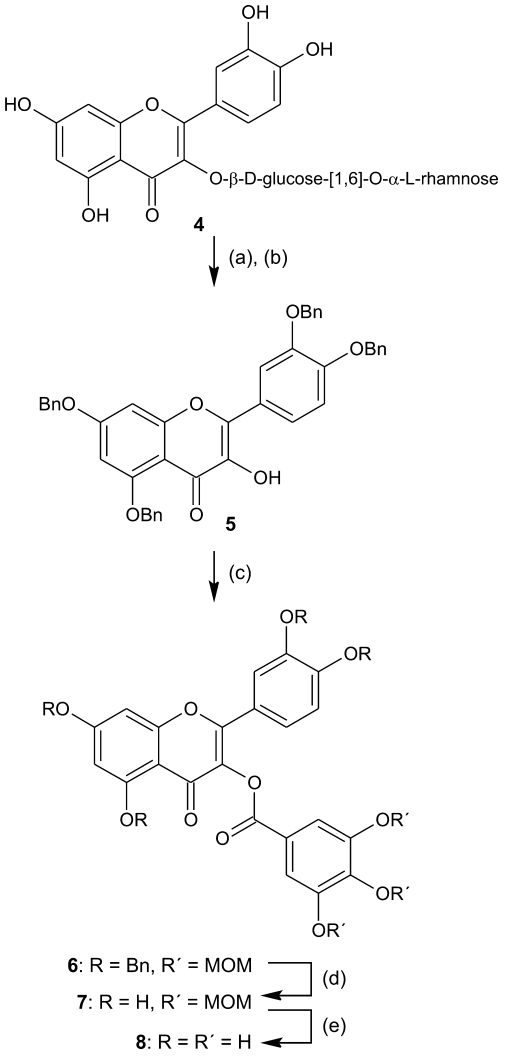

[a]Reagents and conditions: (a) BnBr (6 equiv), Cs_2CO_3 (4.5 equiv), DMF, 44 h at room temp, then 50 °C for 4 h; (b) EtOH/HCl (42:8, v/v), reflux, 2 h, 23% (after two steps); (c) MOM_3gallic acid, DCC/DMAP, CH_2Cl_2, room temp, overnight; (d) H_2−Pd/C, EtOAc, room temp, 4 h, 35% (after steps c and d); (e) MeOH, HCl (cat.), room temp, 3 h, 83%.

quercetin **5** by MOM-protected gallic acid using DCC/DMAP led to an orthogonally protected galloyl ester, which was stepwise deprotected to achieve sufficient purification. The deprotection started by catalytic hydrogenolysis of the benzyl groups using Pd on carbon. The crude product from the hydrogenolysis was then extensively purified by column chromatography to remove all side products. Pure galloyl ester **7** bearing MOM groups protecting the galloyl moiety was then treated with a methanolic solution of HCl, which yielded galloyl ester **8**.

BIOLOGICAL RESULTS

Cytotoxicity of Tested Compounds in RAW264.7 Cells. The effect of the tested compounds (Figure 1) on the viability of RAW264.7 cells was examined using an MTT reduction assay. At concentrations of 10 and 50 μM and 6 h of exposure, the natural flavonoids quercetin, isoquercitrin, and taxifolin caused negligible changes in cell viability (Figure 2). In contrast, the newly synthesized galloyl esters and free gallic acid showed moderate cytotoxicity. For instance, 6 h of cell exposure to 50 μM 3-*O*-galloylquercetin, 7-*O*-galloyltaxifolin, or gallic acid significantly decreased cell viability to 79%, 72%, and 76%, respectively (Figure 2).

7-*O*-Galloyltaxifolin Is Converted to 7-*O*-Galloylquercetin in RAW264.7 Cells. Prior to the expression studies, the stability of the galloylated derivatives during the cell treatment was examined by the HPLC/MS method. On a phenyl-based HPLC column, 7-*O*-galloyltaxifolin and 3-*O*-galloylquercetin gave well-resolved chromatographic peaks at 10.2 and 10.7 min, respectively (Figure 3). Electrospray ionization/quadrupole time-of-flight mass spectrometry (ESI-QqTOF MS) enabled both compounds to be identified on the basis of their MS fragmentation patterns and elemental composition determination. Using MS with negative ESI, 3-*O*-galloylquercetin and 7-*O*-galloyltaxifolin gave pseudomolecular $[M - H]^-$ peaks at m/z 453.0446 and 455.0599, respectively. The full MS and MS^E spectra of both compounds are shown in Figure 4A,B.

When RAW264.7 cells were incubated for up to 6 h with 50 μM 3-*O*-galloylquercetin or 7-*O*-galloyltaxifolin, the uptake of both compounds was relatively fast. After 10 min of incubation, the intracellular concentrations of both galloyl esters reached approximately 85% of their maximal values, which were found after 3 h of exposure and remained almost unchanged for additional 3 h. For instance, the yield of 3-*O*-galloylquercetin was 1.75 and 1.80 nmol per 10^6 cells after 3 and 6 h of incubation, respectively (data not shown). The chromatogram of the cell extract prepared after 6 h of cell exposure to 50 μM 3-*O*-galloylquercetin is shown in Figure 3 (line d). After the cell

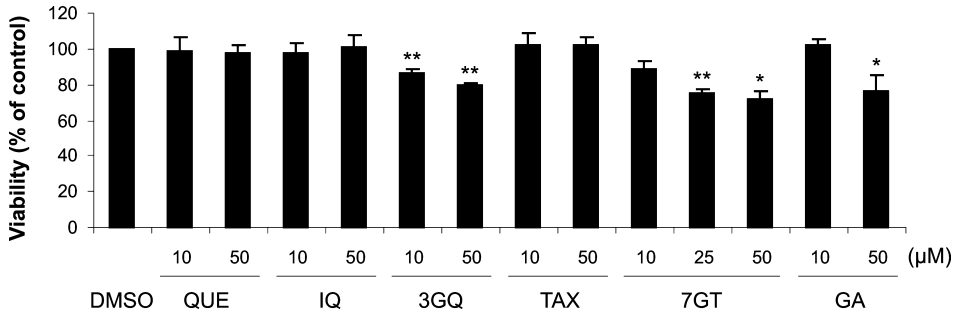

Figure 2. Effect of tested phenolic compounds on viability of RAW264.7 cells. Cells were treated for 6 h with 0.1% DMSO (control) or with indicated concentrations of quercetin (QUE), isoquercitrin (IQ), 3-*O*-galloylquercetin (3GQ), taxifolin (TAX), 7-*O*-galloyltaxifolin (7GT), or gallic acid (GA). The cell viability was determined by MTT reduction assay. Data are means ± SD of three experiments. * $p < 0.05$; ** $p < 0.01$, significantly decreased versus control.

dx.doi.org/10.1021/jm3013344 | *J. Med. Chem.* 2013, 56, 856−866

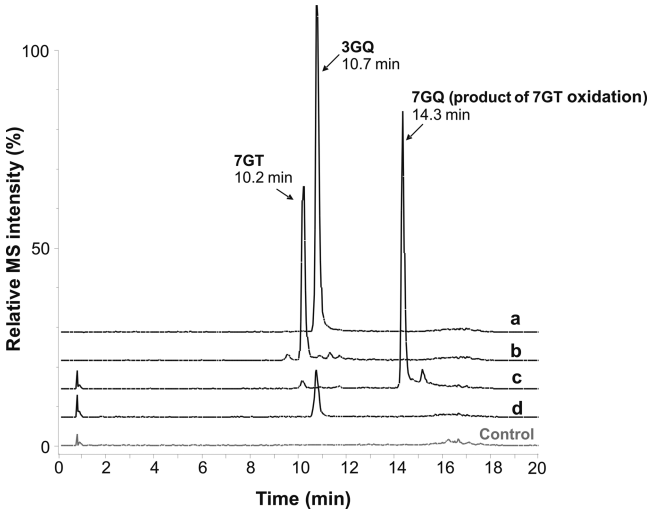

Figure 3. HPLC/MS chromatograms of galloylated derivatives of quercetin and taxifolin. Standard solutions (2 μg/mL) of 3-*O*-galloylquercetin (3GQ, line a) or 7-*O*-galloyltaxifolin (7GT, line b) and extracts of RAW264.7 cells treated for 6 h with 50 μM 7GT (line c), 50 μM 3GQ (line d), or 0.1% DMSO (control) were analyzed by HPLC/ESI-QqTOF MS. The *m*/*z* values of 453 and 455 were monitored using selected-ion monitoring mode. 7GQ, 7-*O*-galloylquercetin (a product of 7GT oxidation).

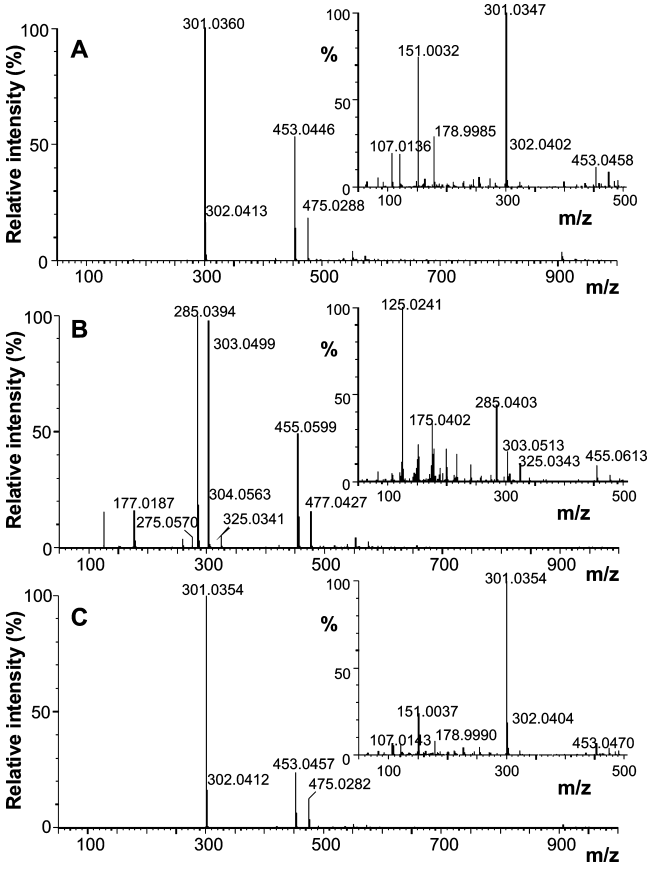

Figure 4. Full MS spectra and MS^E fragmentation (insets) of (A) 3-*O*-galloylquercetin, (B) 7-*O*-galloyltaxifolin, and (C) 7-*O*-galloylquercetin. The MS spectra were obtained from the chromatographic peaks shown in Figure 3. For details on MS fragmentation, see Supporting Information.

treatment, both 3-*O*-galloylquercetin and 7-*O*-galloyltaxifolin were found to be stable with respect to their possible hydrolytic cleavage. HPLC/MS detection of $[M - H]^-$ ions of gallic acid, quercetin, and taxifolin at *m*/*z* 169, 301, and 303, respectively, showed that the levels of gallic acid were undetectable and that the intracellular amounts of quercetin or taxifolin represented less than 4.5% of the respective parent compound. The same quantities of hydrolytic products were also found when stock solutions of 3-*O*-galloylquercetin or 7-*O*-galloyltaxifolin in DMSO were analyzed prior to their addition to the cells (data not shown). In contrast to 3-*O*-galloylquercetin, the treatment of RAW264.7 cells with 7-*O*-galloyltaxifolin resulted in the appearance of a specific product having a peak at 14.3 min (Figure 3, line c). The ESI-QqTOF MS analysis identified this product as 7-*O*-galloylquercetin. As shown in Figure 4, the MS and MS^E spectra of 7-*O*-galloylquercetin (Figure 4C) were essentially the same as those of 3-*O*-galloylquercetin (Figure 4A). The formation of 7-*O*-galloylquercetin was not observed after the incubation of the parent compound in the culture medium without RAW264.7 cells. These results showed that the cells were responsible for the oxidation of 7-*O*-galloyltaxifolin to 7-*O*-galloylquercetin, with the product detected in cells as early as 10 min after the start of the cell treatment. After 3 h of cell exposure to 50 μM 7-*O*-galloyltaxifolin, the content of 7-*O*-galloyltaxifolin and 7-*O*-galloylquercetin was 1.03 and 8.08 nmol per 10^6 cells, respectively, and very similar ratios between the parent compound and product were found, regardless of the incubation time (data not shown).

Exposure to 7-*O*-Galloyltaxifolin Increases mRNA and Protein Levels of Heme Oxygenase-1. The study further investigated the effect of the tested compounds on the expression of the Nrf2 target gene *Hmox1* encoding heme oxygenase-1. As expected, quantitative real-time PCR analysis demonstrated an induction of mouse *Hmox1* gene expression in RAW264.7 cells exposed to quercetin, which was used as a positive control.[15,16] After 6 h of cell exposure, 50 μM quercetin significantly increased the level of Hmox1 mRNA to 4.3-fold when normalized to Gapdh mRNA (Figure 5). A dose-dependent increase in the expression of Hmox1 mRNA was also found after 6 h of cell treatment with 7-*O*-galloyltaxifolin, which appeared to be a more potent *Hmox1* inducer than quercetin. At concentrations of 25 and 50 μM, 7-*O*-galloyltaxifolin significantly elevated Hmox1 mRNA levels to

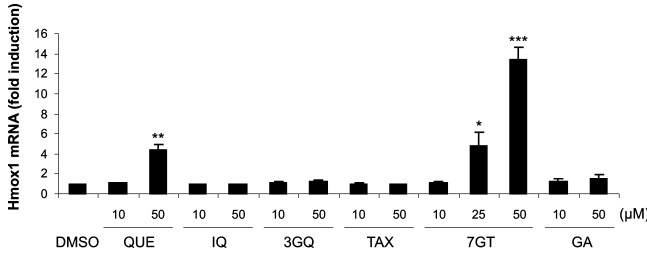

Figure 5. Relative changes in *Hmox1* gene expression by tested phenolic compounds in RAW264.7 cells. Cells were treated for 6 h with 0.1% DMSO (control) or with indicated concentrations of quercetin (QUE), isoquercitrin (IQ), 3-*O*-galloylquercetin (3GQ), taxifolin (TAX), 7-*O*-galloyltaxifolin (7GT), or gallic acid (GA). The levels of Hmox1 mRNA were determined by quantitative real-time PCR with results normalized to Gapdh mRNA. Data are means ± SD of three experiments. * $p < 0.05$; ** $p < 0.01$; *** $p < 0.001$, significantly increased versus control.

dx.doi.org/10.1021/jm3013344 | J. Med. Chem. 2013, 56, 856−866

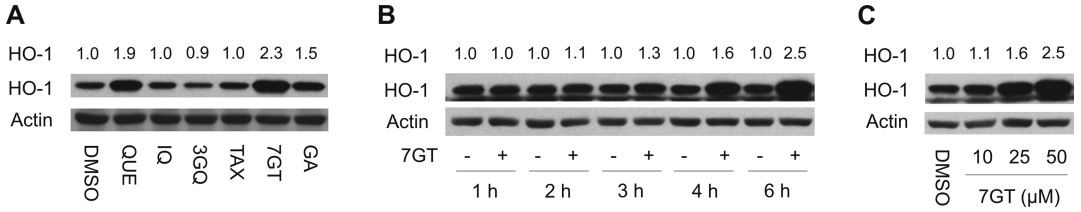

Figure 6. Effect of tested phenolic compounds on heme oxygenase-1 (HO-1) protein levels in RAW264.7 cells. (A) Cells were treated for 6 h with 0.1% DMSO (control) or with 50 μM quercetin (QUE), isoquercitrin (IQ), 3-*O*-galloylquercetin (3GQ), taxifolin (TAX), 7-*O*-galloyltaxifolin (7GT), or gallic acid (GA). (B) Cells were incubated for 1−6 h in the absence or presence of 50 μM 7GT (as indicated). (C) Cells were treated for 6 h with 0.1% DMSO (control) or with 10 to 50 μM 7GT. After treatment, proteins in the whole cell lysates (20 μg/lane) were analyzed by Western blotting and HO-1 and actin were visualized by chemiluminescent detection. Relative HO-1 band intensities normalized to actin are shown. Data are means of three experiments.

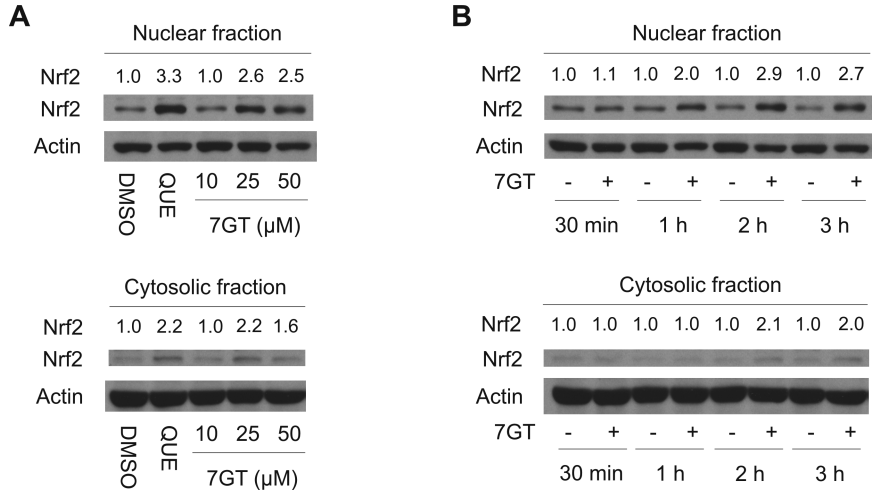

Figure 7. Effect of 7-*O*-galloyltaxifolin (7GT) on nuclear and cytosolic levels of Nrf2 in RAW264.7 cells. (A) Cells were treated for 3 h with 0.1% DMSO (control), 50 μM quercetin (QUE; positive control), or 10−50 μM 7GT. (B) Cells were incubated for 30 min to 3 h in the absence or presence of 50 μM 7GT (as indicated). After treatment, cells were fractionated, and the proteins in nuclear and cytosolic fractions (30 μg/lane) were analyzed by Western blotting. Nrf2 and actin were visualized by chemiluminescent detection. Relative Nrf2 band intensities normalized to actin are shown. Data are means of three experiments.

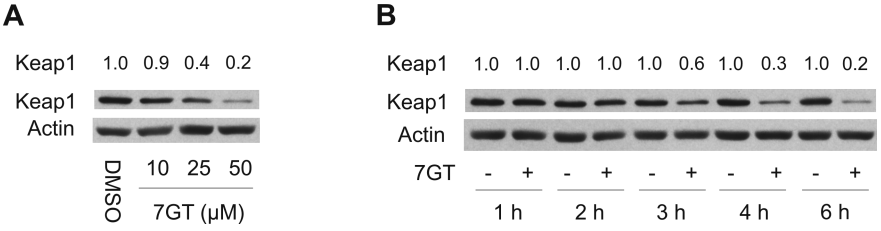

Figure 8. Effect of 7-*O*-galloyltaxifolin (7GT) on Keap1 protein levels in RAW264.7 cells. (A) Cells were treated for 6 h with 0.1% DMSO (control) or with 10−50 μM 7GT. (B) Cells were incubated for 1−6 h in the absence or presence of 50 μM 7GT (as indicated). After treatment, proteins in the whole cell lysates (20 μg/lane) were analyzed by Western blotting, and Keap1 and actin were visualized by chemiluminescent detection. Relative Keap1 band intensities normalized to actin are shown. Data are means of three experiments.

4.8-fold and 13.4-fold, respectively, compared with the control (Figure 5). This aside, 6 h of exposure to 50 μM gallic acid produced a small, statistically nonsignificant increase in the level of Hmox1 mRNA that reached (1.5 ± 0.3)-fold that of the control. In contrast, the expression of Hmox1 mRNA remained practically unaffected in cells treated with isoquercitrin, 3-*O*-galloylquercetin, or taxifolin (Figure 5).

The levels of Hmox1 mRNA appeared to correlate with the abundance of heme oxygenase-1 (HO-1) protein. In RAW264.7 cells treated for 6 h with individual tested compounds (50 μM), Western blot analysis showed an obvious upregulation of HO-1 by quercetin and 7-*O*-galloyltaxifolin (Figure 6A). A slight increase in the protein level of HO-1 was also induced by gallic acid, whereas no substantial changes in the expression of HO-1 were found after cell exposure to isoquercitrin, 3-*O*-galloylquercetin, or taxifolin (Figure 6A). The upregulation of HO-1 by 7-*O*-galloyltaxifolin was both time- and dose-dependent. At a concentration of 50 μM, the increased abundance of HO-1 was detected as early as 3 h after the start of the incubation (Figure 6B). After 6 h of cell treatment, 7-*O*-galloyltaxifolin clearly elevated the protein levels of HO-1 at concentrations of 25 μM and above (Figure 6C).

Exposure to 7-*O*-Galloyltaxifolin Induces Nuclear Accumulation of Nrf2 and Downregulates Keap1. To characterize the mechanisms by which 7-*O*-galloyltaxifolin induces *Hmox1* gene expression, the nuclear and cytosolic

dx.doi.org/10.1021/jm3013344 | J. Med. Chem. 2013, 56, 856−866

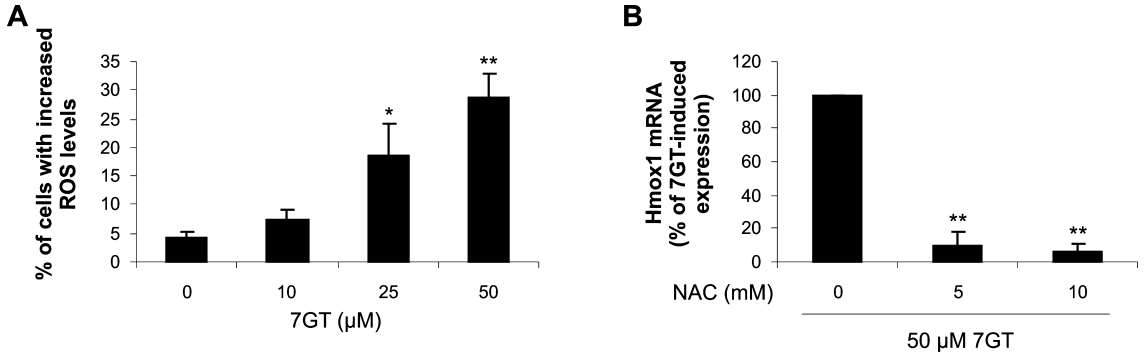

Figure 9. ROS generation by 7-*O*-galloyltaxifolin (7GT) and effect of *N*-acetyl-L-cysteine (NAC) on 7GT-induced *Hmox1* gene expression in RAW264.7 cells. (A) Cells were treated for 2 h with 10−50 μM 7GT. After treatment, cells were incubated with carboxy-H_2DCFDA and the percentage of cells with increased ROS levels was evaluated by flow cytometry. Data are means ± SD of three experiments. * $p < 0.05$; ** $p < 0.01$, significantly increased versus control. (B) Cells were pretreated for 30 min with 5 or 10 mM NAC and then incubated in the absence or presence of 50 μM 7GT for additional 6 h. The levels of Hmox1 mRNA were determined by quantitative real-time PCR and normalized to Gapdh mRNA. Results are expressed as the percentage of 7GT-induced Hmox1 mRNA expression. Data are means ± SD of three experiments. ** $p < 0.01$, significantly different from cells treated with 7GT in the absence of NAC.

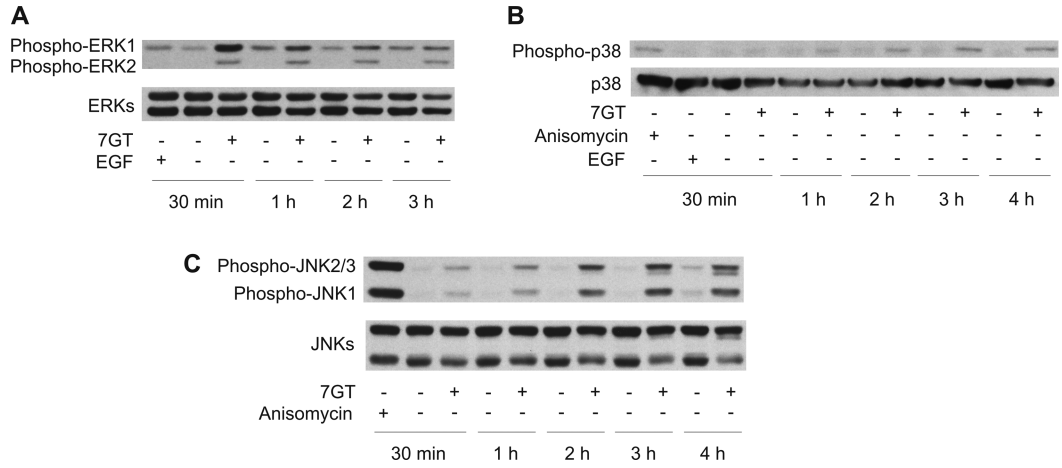

Figure 10. Effect of 7-*O*-galloyltaxifolin (7GT) on the phosphorylation status of MAPKs in RAW264.7 cells. (A) Cells were treated for 30 min with 75 ng/mL epidermal growth factor (EGF; positive control) or incubated for 30 min to 3 h in the absence or presence of 50 μM 7GT (as indicated). After treatment, proteins in the whole cell lysates (20 μg/lane) were analyzed by Western blotting. ERK1 phosphorylated at Thr202 and Tyr204, ERK2 phosphorylated at Thr185 and Tyr187, and total ERK1/2 were visualized by chemiluminescent detection. (B) Cells were treated for 30 min with 5 μM anisomycin (positive control) or 75 ng/mL EGF or incubated for 30 min to 4 h in the absence or presence of 50 μM 7GT (as indicated). The levels of p38 MAPKs dually phosphorylated at Thr180/Tyr182 and total p38 MAPKs were analyzed in the whole cell lysates (35 μg/lane) as mentioned above. (C) Cells were treated for 30 min with 5 μM anisomycin (positive control) or incubated for 30 min to 4 h in the absence or presence of 50 μM 7GT (as indicated). JNKs dually phosphorylated at Thr183/Tyr185 and total JNKs were analyzed in the whole cell lysates (30 μg/lane) as mentioned above.

levels of the transcription factor Nrf2 were analyzed by Western blotting. The treatment of RAW264.7 cells for 3 h with 50 μM quercetin, a positive control,[8] elevated the protein levels of Nrf2 in both nuclear and cytosolic fractions (Figure 7A). After 3 h of exposure, 7-*O*-galloyltaxifolin was found to increase the levels of Nrf2 in both fractions at concentrations of 25 and 50 μM (Figure 7A). A time-course experiment revealed that 50 μM 7-*O*-galloyltaxifolin elevated the nuclear levels of Nrf2 as early as 1 h after the start of the incubation, while the cytosolic Nrf2 levels slightly increased after 2 h (Figure 7B). These results demonstrated that 7-*O*-galloyltaxifolin was able to enhance the nuclear accumulation of Nrf2 as well as the total cellular Nrf2 content. We also tested whether the upregulation of Nrf2 by 7-*O*-galloyltaxifolin could be associated with the degradation of Keap1, a negative regulator of Nrf2.[7] Western blot analysis of whole cell lysates showed that 7-*O*-galloyltaxifolin dose-dependently reduced the protein levels of Keap1 after 6 h of treatment (Figure 8A). At a concentration of 50 μM, the effect of 7-*O*-galloyltaxifolin was also found to be time-dependent, while the levels of Keap1 started to decline after 3 h of incubation (Figure 8B). Our results showed that the nuclear accumulation of Nrf2 preceded the downregulation of Keap1, and hence other mechanisms of 7-*O*-galloyltaxifolin-induced *Hmox1* gene expression needed to be taken into account.

Antioxidant *N*-Acetyl-L-cysteine Suppresses 7-*O*-Galloyltaxifolin-Induced *Hmox1* Gene Expression. To evaluate possible involvement of reactive oxygen species (ROS) in the modulation of *Hmox1* gene expression by 7-*O*-galloyltaxifolin, we first examined whether cell exposure to 7-*O*-galloyltaxifolin caused ROS generation. Flow cytometric analysis using a carboxy derivative of reduced and acetylated 2′,7′-dichlorofluorescein showed that exposure of RAW264.7 cells to a potent prooxidant, *tert*-butyl hydroperoxide (TBHP),

dx.doi.org/10.1021/jm3013344 | J. Med. Chem. 2013, 56, 856−866

induced an increase in the cell fluorescence, indicative of intracellular ROS production.[17] Increased levels of ROS were detected in 3−5% of untreated cells and in 25% ± 4% of cells treated for 30 min with 100 μM TBHP (data not shown). When the cells were exposed to 7-*O*-galloyltaxifolin, elevated ROS levels were found after 2 h of exposure. At concentrations of 25 and 50 μM, 7-*O*-galloyltaxifolin raised the cell population with increased ROS levels to 19% and 29%, respectively (Figure 9A). We further examined whether the induction of *Hmox1* gene expression by 7-*O*-galloyltaxifolin could be reduced by a nonspecific ROS scavenger *N*-acetyl-L-cysteine (NAC).[10] We found that 30 min pretreatment of RAW264.7 cells with 5 or 10 mM NAC, neutralized with sodium bicarbonate, significantly decreased Hmox1 mRNA levels induced by 50 μM 7-*O*-galloyltaxifolin at 6 h of exposure by 90% and 94%, respectively (Figure 9B). Moreover, we also found that 5 and 10 mM NAC did not prevent the oxidation of 7-*O*-galloyltaxifolin to 7-*O*-galloylquercetin (data not shown). These results suggest that ROS are responsible for the induction of *Hmox1* gene expression by 7-*O*-galloyltaxifolin and that 7-*O*-galloylquercetin is produced enzymatically rather than through a chemical process.

Induction of *Hmox1* Gene Expression by 7-*O*-Galloyltaxifolin Involves the Activities of p38 MAPKs and ERKs. Since ROS activate MAPK cascades,[18] the study examined the possible involvement of MAPKs in the induction of Hmox1 mRNA expression by 7-*O*-galloyltaxifolin. The activity of MAPKs is regulated by upstream activating kinases and inactivating protein phosphatases.[19] Therefore, we first tested the effect of 7-*O*-galloyltaxifolin on the phosphorylation status of MAPKs. As shown by Western blotting with phospho-specific antibodies, epidermal growth factor (EGF) and anisomycin were appropriate positive controls[20] for stimulating the phosphorylation of MAPKs in RAW264.7 cells. After 30 min of treatment, 75 ng/mL EGF increased the phosphorylation of ERK1 but not ERK2 (Figure 10A). In contrast, 30 min of exposure to 5 μM anisomycin enhanced the phosphorylation of p38 MAPKs (Figure 10B) and JNKs (Figure 10C). Cell treatment for 30 min with 50 μM 7-*O*-galloyltaxifolin caused a marked increase in the phosphorylation of both ERK1 and ERK2. The levels of phosphorylated ERK1/2 decreased somewhat with further incubation but remained above basal levels for up to 3 h (Figure 10A). This aside, 7-*O*-galloyltaxifolin was found to elevate the phosphorylation of p38 MAPKs and JNKs in a time-dependent manner. The levels of phosphorylated p38 MAPKs were slightly elevated by 50 μM 7-*O*-galloyltaxifolin after 1 h of cell exposure (Figure 10B), while the increased phosphorylation of JNKs was detected as early as 30 min after start of the incubation (Figure 10C). Since 7-*O*-galloyltaxifolin increased the phosphorylation of all three MAPK subfamilies, we subsequently employed specific pharmacological MAPK inhibitors PD98059, SB203580, and SP600125 to suppress the activity of ERKs, p38 MAPKs, and JNKs, respectively.[15] Our results showed that the increase in Hmox1 mRNA induced by 7-*O*-galloyltaxifolin was significantly reduced by the inhibitors of ERKs and p38 MAPKs. Pretreatment of RAW264.7 cells for 30 min with 15 μM PD98059 or 15 μM SB203580 decreased the induction of Hmox1 mRNA by 6 h of exposure to 50 μM 7-*O*-galloyltaxifolin by 15% and 70%, respectively (Figure 11). In contrast, the inhibition of JNKs by 30 μM SP600125 enhanced the effect of 7-*O*-galloyltaxifolin on Hmox1 mRNA level by 90% under the same experimental conditions (Figure 11).

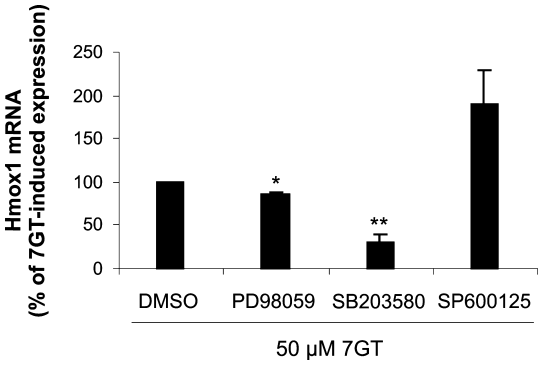

Figure 11. Effect of MAPK inhibitors on 7-*O*-galloyltaxifolin (7GT)-induced *Hmox1* gene expression in RAW264.7 cells. Cells were pretreated for 30 min with 0.1% DMSO (control), 15 μM PD98059, 15 μM SB203580, or 30 μM SP600125 and then incubated in the absence or presence of 50 μM 7GT for additional 6 h. The levels of Hmox1 mRNA were determined by quantitative real-time PCR and normalized to Gapdh mRNA. Results are expressed as the percentage of 7GT-induced Hmox1 mRNA expression. Data are means ± SD of three experiments. * $p < 0.05$; ** $p < 0.01$, significantly different from cells treated with 7GT in the absence of MAPK inhibitors.

DISCUSSION

The natural flavonoids quercetin and taxifolin (dihydroquercetin) exhibit a wide range of biological activities, e.g. antioxidative, anti-inflammatory, and anticancer.[13,14,21] The molecules of both flavonoids may also serve as the backbone for a number of potentially bioactive derivatives, such as the glycosides produced in plants[22,23] or glucuronides, sulfates, and methyl conjugates produced by phase II xenobiotic metabolizing enzymes.[24] This aside, semisynthetic 3-*O*-acylquercetins with aliphatic acyl groups having 2−16 carbon atoms have been characterized.[25] In this study, we prepared galloylated derivatives of quercetin and taxifolin and examined their effect on the Nrf2 signaling pathway, which regulates the expression of genes encoding many cytoprotective and stress-responsive enzymes, including heme oxygenase-1 (HO-1).[4] We synthesized two galloyl esters, namely, 3-*O*-galloylquercetin and 7-*O*-galloyltaxifolin. These compounds have not been identified in plants to date, even though plants contain gallic acid both in the free form and esterified to sugars, for example, in tannins, and to certain flavonoids such as catechins and proanthocyanidins.[23] Previous studies have shown that quercetin[8] and gallic acid activate the Nrf2 signaling pathway.[26] Quercetin has been consistently found to induce HO-1 expression in several cell models.[15,27] Upregulation of HO-1 has also been demonstrated in the hearts of rats that were orally administered gallic acid.[28] HO-1 is a highly inducible enzyme that catalyzes the degradation of heme into ferrous ion, the antioxidant biliverdin, and anti-inflammatory agent carbon monoxide. The modulation of HO-1 activity may hence represent a potential therapeutic target for the treatment of diseases associated with inflammation and oxidative stress, such as inflammatory bowel disease[29] and atherosclerosis.[30]

Our study on murine macrophage RAW264.7 cells confirms the upregulation of HO-1 expression by quercetin and to a lesser extent by gallic acid as well. In contrast, the expression of HO-1 was unaffected by quercetin 3-*O*-conjugates, including the semisynthetic galloyl ester 3-*O*-galloylquercetin and natural glycoside isoquercitrin (quercetin-3-*O*-glucoside). Similarly to isoquercitrin, the other quercetin glycosides, quercitrin

(quercetin-3-*O*-rhamnoside) and rutin (quercetin-3-*O*-rhamnoglucoside), were also found to be unable to induce the expression of HO-1 in RAW264.7 cells.[15] In our study, the expression of HO-1 also remained unchanged by taxifolin, which only differs from quercetin in the absence of a 2,3-double bond. The inactivity of taxifolin agreed with previous results obtained from the retinal ganglion RGC-5 cell line.[31] On the other hand, we report here that galloylation of the 7-OH group in taxifolin provided a novel HO-1 inducer, 7-*O*-galloyltaxifolin, which was found to increase both the mRNA and protein levels of HO-1 at concentrations from 25 μM upward. HPLC/MS analyses showed that 7-*O*-galloyltaxifolin was readily absorbed by RAW264.7 cells and that the galloyl ester was stable with respect to its possible hydrolytic cleavage. In contrast, a rapid establishment of the equilibrium between the absorbed 7-*O*-galloyltaxifolin and its oxidation product 7-*O*-galloylquercetin was found, with an approximate parent compound/product ratio of 1/8. To date, several plant enzymes including flavonol synthase, anthocyanidin synthase,[32] and horseradish peroxidase[33] have been shown to catalyze the oxidation of dihydroquercetin to quercetin. The mechanism of the dihydroquercetin skeleton oxidation in the structure of 7-*O*-galloyltaxifolin presented herein remains unclear. Nonetheless, the presence of the galloyl moiety seems to be important, because ungalloylated taxifolin was found not to be oxidized to quercetin in animal cells.[24,34] Since both 7-*O*-galloyltaxifolin and its oxidation product 7-*O*-galloylquercetin were simultaneously present in RAW264.7 cells soon after the start of the cell treatment, we were unable to determine which member of the redox couple was responsible for the biological response. Nrf2 is the primary transcription factor involved in the induction of antioxidant response element-driven gene expression.[4] The upregulation of Nrf2 activity is associated with the nuclear accumulation of Nrf2, arising either from the degradation of Keap1, a negative regulator of Nrf2, or from the phosphorylation of Nrf2 by protein kinases.[7] We demonstrated that the induction of HO-1 expression by 7-*O*-galloyltaxifolin was almost completely suppressed by the antioxidant *N*-acetylcysteine, suggesting involvement of ROS in mediating the biological effect of 7-*O*-galloyltaxifolin. ROS are known to activate different classes of MAPKs.[18] Our experiments revealed that cell treatment with 7-*O*-galloyltaxifolin induced prompt phosphorylation of p38 MAPKs, ERK1/2, and JNKs, followed by the nuclear accumulation of Nrf2. Moreover, we found that the induction of HO-1 by 7-*O*-galloyltaxifolin required the activities of p38 MAPKs and ERKs but not JNKs, since pharmacological inhibitors of p38 MAPKs and ERKs decreased 7-*O*-galloyltaxifolin-induced mRNA levels of HO-1 by 70% and 15%, respectively. These results suggest that the introduction of a galloyl moiety into the molecule of taxifolin brings about the ability to induce ROS production and MAPK activation. Although 7-*O*-galloyltaxifolin also downregulated Keap1, this event occurred later than the nuclear accumulation of Nrf2. We may therefore presume that the downregulation of Keap1 was not the primary reason for 7-*O*-galloyltaxifolin-induced HO-1 expression, but the decrease in Keap1 levels could potentiate the effect of 7-*O*-galloyltaxifolin during longer treatments. Our results show that 7-*O*-galloyltaxifolin induces HO-1 expression primarily through the activation of protein kinase cascades. Similarly, it has also been demonstrated that the upregulation of HO-1 by quercetin involves the activation of the ERK1/2 and p38 MAPK pathways[15,27] and the effect of epigallocatechin-3-gallate on HO-1 expression has been linked with the activation of the phosphoinositide 3-kinase/Akt and ERK1/2 pathways.[10]

In summary, we have shown that galloylation or glycosylation of the 3-OH group in quercetin removes its ability to induce HO-1 expression in RAW264.7 cells. In contrast, we have prepared a novel HO-1 inducer by galloylation of the 7-OH group in taxifolin. The mechanism of 7-*O*-galloyltaxifolin-induced HO-1 expression involves the generation of ROS and phosphorylation of p38 MAPKs and ERK1/2, which are associated with activation of the Nrf2 signaling pathway. Since 7-*O*-galloyltaxifolin is oxidized to 7-*O*-galloylquercetin in RAW264.7 cells, further research should be aimed at synthesizing 7-*O*-galloylquercetin and evaluating its effect on the Nrf2 pathway.

EXPERIMENTAL SECTION

Chemistry: General Methods. NMR spectra were recorded on a Bruker Avance III 600 MHz spectrometer (Bruker Daltonics, Billerica, MA, USA; 600.23 MHz for ^{1}H, 150.93 MHz for ^{13}C at 30 °C) in DMSO-d_6 (99.9 atom % D; Sigma-Aldrich, Steinheim, Germany). Residual signal of solvent was used as an internal standard (δ_H 2.500 ppm, δ_C 39.60 ppm). NMR experiments: ^{1}H NMR, ^{13}C NMR, gCOSY, gHSQC, and gHMBC were performed using the manufacturer's software. ^{1}H NMR and ^{13}C NMR spectra were zero filled to 4-fold data points and multiplied by window function before Fourier transformation. Two-parameter double-exponential Lorentz−Gauss function was applied for ^{1}H to improve resolution and line broadening (1 Hz) was applied to get better ^{13}C signal-to-noise ratio. Chemical shifts are given in δ-scale with digital resolution justifying the reported values to three (δ_H) or two (δ_C) decimal places.

ESI-MS spectra were measured with Micromass LC-MS Platform in MeOH with addition of HCO_2H; HRMS spectra (ESI, APCI, FAB) were measured with a LTQ Orbitrap XL instrument (Thermo Fisher Scientific, Waltham, MA, USA) or with a ZAB-EQ instrument (VG Analytical, Manchester, UK).

Purity of the tested compounds was determined by HPLC, and in all cases, the purity reached at least 95% (for respective chromatograms, see Supporting Information). HPLC analyses were carried out using a Shimadzu Prominence LC analytical system consisting of LC-20AD binary HPLC pump, SIL-20AC cooling autosampler, CTO-10AS column oven, and SPD-20MA diode array detector (Shimadzu, Kyoto, Japan). A Chromolith Performance RP-18e monolithic column (100 mm × 3 mm) equipped with a guard column (5 mm × 4.6 mm) (Merck, Darmstadt, Germany) was used with an isocratic mobile phase CH_3CN/MeOH/H_2O/TFA (2:37:61:0.1, flow rate 1.8 mL/min) at 25 °C and UV detection at 285 nm (+ scan 200−365 nm).

*7-O-Galloyltaxifolin (**3**).* Taxifolin (**1**; 250 mg, 0.821 mmol) and 3,4,5-tri-*O*-benzylgalloyl chloride (568 mg, 1.239 mmol) were dissolved in dry pyridine (10 mL) and stirred at 0 °C for 1 h. The reaction was stopped by diluting in ice-cold HCl (1 M, 75 mL), the solution was extracted with EtOAc (2 × 50 mL), and the organic layers were combined, dried (Na_2SO_4), evaporated, and chromatographed ($CHCl_3$/acetone/HCO_2H, 95:5:1) to yield 7-*O*-(3′,4′,5′-tri-*O*-benzylgalloyl)taxifolin (**2**, 138 mg, 23%) as a white amorphous solid (ESI-MS (m/z) 749 $[M + Na]^+$; for ^{1}H and ^{13}C NMR data see Tables S1 and S2 in Supporting Information). Compound **2** (100 mg, 0.138 mmol) was dissolved in EtOAc (10 mL) and then Pd/C (100 mg, 10% Pd) was added and stirred under H_2 for 3 h (20 °C). The Pd was then removed by filtration through Celite, which was washed with acetone, and the solvent was evaporated. Flash chromatography ($CHCl_3$/MeOH/HCO_2H, 9:1:0.1) yielded title compound **3** (59 mg, 94%) as a white amorphous solid. HRMS calcd $[M + Na]^+$ 479.0585, found 479.0583. ^{1}H NMR (600.23 MHz, DMSO-d_6, 30 °C): δ 4.771 (d, 1H, J = 11.7, H-3), 5.172 (d, 1H, J = 11.7, H-2), 6.417 (d, 1H, J = 2.1, H-8), 6.450 (d, 1H, J = 2.1, H-6), 6.867 (d, 1H, J = 8.1, H-5′), 6.936 (dd, 1H, J = 2.1, 8.1, H-6′), 7.101 (d, 1H, J = 2.1, H-2′), 7.214 (s, 2H, Gal *o*-CH). ^{13}C NMR (150.93 MHz, DMSO-d_6, 30 °C): δ 74.14 (C-3), 85.42 (C-2), 103.31 (C-8), 104.44 (C-6), 106.01 (C-4a), 111.21 (Gal

dx.doi.org/10.1021/jm3013344 | J. Med. Chem. 2013, 56, 856−866

ortho), 116.49 (C-5′), 116.58 (C-2′), 120.35 (Gal *ipso*), 121.55 (C-6′), 130.01 (C-1′), 141.22 (Gal *para*), 146.50 (C-3′), 147.22 (Gal *meta*), 147.42 (C-4′), 161.05 (C-7), 164.30 (C-5), 164.30 (C-8a), 165.22 (Gal C═O), 200.72 (C-4). Gal = galloyl moiety.

*3-O-Galloylquercetin (**8**).* 3-*O*-[(3″,4″,5″-Tri-*O*-methoxymethyl)-galloyl]quercetin (**7**; 250 mg, 0.426 mmol, for the preparation see Supporting Information) was dissolved in MeOH (15 mL), concentrated HCl (1 mL) was added, and the resulting mixture was stirred at room temperature for 3 h. The reaction was quenched by the addition of a saturated solution of $NaHCO_3$ (till neutral pH), evaporated to dryness by coevaporation with absolute EtOH, redissolved in acetone, filtered to remove inorganic salts, and evaporated again. The dry residue yielded title compound **8** (160 mg, 83%) after flash chromatography ($CHCl_3$/MeOH/HCO_2H, from 95:5:1 to 90:10:1). HRMS calcd $[M + Na]^+$ 477.0428, found 477.0427. ^1H NMR (600.23 MHz, DMSO-d_6, 30 °C): δ 6.197 (d, 1H, J = 2.0, H-6), 6.435 (d, 1H, J = 2.0, H-8), 6.829 (d, 1H, J = 8.4, H-5′), 7.214 (s, 2H, Gal *o*-CH), 7.262 (dd, 1H, J = 2.3, 8.4, H-6′), 7.348 (d, 1H, J = 2.3, H-2′). ^{13}C NMR (150.93 MHz, DMSO-d_6, 30 °C): δ 94.32 (C-8), 99.51 (C-6), 102.83 (C-4a), 109.34 (Gal *ortho*), 114.87 (C-2′), 115.81 (C-5′), 116.62 (Gal *ipso*), 119.45 (C-1′), 120.40 (C-6′), 129.79 (C-3), 140.73 (Gal *para*), 145.80 (C-3′), 145.97 (Gal *meta*), 149.98 (C-4′), 155.85 (C-2), 156.81 (C-8a), 161.11 (C-5), 163.38 (Gal C═O), 166.45 (C-7), 174.90 (C-4). Gal = galloyl moiety.

Biological Testing. *Reagents.* Quercetin, gallic acid, anisomycin, *N*-acetyl-L-cysteine, PD98059 (2-(2-amino-3-methoxyphenyl)-4*H*-1-benzopyran-4-one), SB203580 (4-(4-fluorophenyl)-2-(4-methylsulfinylphenyl)-5-(4-pyridyl)-1*H*-imidazole), SP600125 (1,9-pyrazoloanthrone), human epidermal growth factor, and dimethyl sulfoxide (DMSO) were purchased from Sigma-Aldrich (St. Louis, MO, USA). Taxifolin was obtained from Amagro (Prague, Czech Republic). Isoquercitrin (98% purity, HPLC) was prepared by the enzymatic procedure as described previously.[35] Nitrogen, argon, and helium (all 99.999%) were obtained from Linde Gas (Prague, Czech Republic). Water for HPLC was prepared using an Ultrapur reverse osmosis-deionizer system (Watrex, Prague, Czech Republic).

RAW264.7 Cell Culture and Treatment. The murine macrophage RAW264.7 cell line (No. 91062702, ECACC, Salisbury, U.K.) was cultured at 37 °C in Dulbecco's modified Eagle's medium (D5796, Sigma) supplemented with 100 U/mL penicillin, 100 μg/mL streptomycin (Invitrogen, Carlsbad, CA, USA), and 10% fetal bovine serum (Biochrom, Berlin, Germany) in a humidified atmosphere containing 5% CO_2. Cells were regularly subcultured before confluence. For all experiments, RAW264.7 cells at passage 5−25 were seeded in the complete culture medium into 6-well plates at a density of 1×10^5 cells/cm^2. After 8 h of stabilization, the culture medium was exchanged for the serum-free medium. After overnight incubation, cells were treated in serum-free medium with the tested compounds. Negative controls were treated with 0.1% (v/v) DMSO only.

Cell Viability Assay. After treating RAW264.7 cells with 0.1% DMSO (control), the tested compounds or 1.5% (v/v) Triton X-100 (positive control), the cell viability was determined using an MTT reduction assay. In brief, cells were washed with PBS and incubated for 2 h at 37 °C in fresh serum-free medium containing 0.5 mg/mL MTT (Sigma). After this, the medium was removed, and the intracellular formazan produced by active mitochondria was solubilized in DMSO. The absorbance at 540 nm was measured on a spectrophotometric plate reader and used to calculate relative cell viability, where cells treated with DMSO alone represented 100% viability.

HPLC/MS Analysis. After treatment, RAW264.7 cells were scraped from the plates, collected by gentle centrifugation, washed twice with PBS, resuspended in 0.4 mL of methanol containing 5% (v/v) acetic acid and sonicated 10 times at 50% amplitude with a cycle set at 0.5 s using an Ultrasonic Processor UP200s equipped with a Sonotrode Microtip S2 sonicator probe (Hielscher, Teltow, Germany). Afterward, the cell lysates were centrifuged for 2 min at 14 000 × g at room temperature, and the supernatants were analyzed by HPLC/MS. Aliquots of culture medium were diluted (1:1, v/v) in methanol containing 5% (v/v) acetic acid, centrifuged for 2 min at 14 000 × g, and the supernatants were analyzed by HPLC/MS. The chromatographic separation was performed in an Agilent Zorbax Eclipse XDB-phenyl column (150 mm × 2.1 mm i.d., 5 μm; Agilent Technologies, CA, USA) using an Acquity UPLC system (Waters, Milford, MA, USA) equipped with a binary solvent manager, sample manager, column manager, and photodiode array detector. The autosampler was conditioned at 4 °C, and the injection volume was 5 μL. A binary gradient elution was performed at a flow rate of 0.4 mL/min; column temperature was maintained at 35 °C. Solvent A was composed of water with 1% (v/v) acetic acid and methanol (90:10, v/v), and solvent B was methanol. The gradient profile was as follows: 0−14 min 10−50% B, 14−16 min 50−100% B, 16−18 min 100−10% B, 18−20 min 10% B. The Waters QqTof Premier mass spectrometer (Waters, Manchester, U.K.) was connected to the UPLC system via an electrospray ionization (ESI) interface. The ESI source operated in negative ionization mode with the capillary voltage at 2.1 kV and the sampling cone at 40 V. The source temperature and the desolvation temperature were set to 120 and 300 °C, respectively. The cone and desolvation gas flows were 0 and 500 L/h, respectively. Data were acquired from 50 to 1000 Da with a 0.5 s scan time. Data acquisition was achieved using two interleaved scan functions (MS and MS^E experiments), which enabled the simultaneous acquisition of both low collision energy and high collision energy mass spectra from a single experiment. The collision energy was set to 5 V for Function 1 and 20−35 V for Function 2. Acquiring data in this manner enabled the collection of intact precursor ions as well as fragment ion information in an unbiased manner. Postacquisition processing of the data was performed using the program Metabolynx V4.1 (Waters, Milford, MA, USA).

Reverse Transcription and Quantitative Real-Time PCR. After treatment, total RNA was extracted using TRI Reagent Solution (Applied Biosystems, Foster City, CA, USA), and the concentration of RNA was determined by spectrophotometry at 260 nm. RNA samples (2 μg) were reverse transcribed using a High Capacity cDNA Reverse Transcription Kit (Applied Biosystems) and real-time PCR was performed in a LightCycler 480 II system (Roche Diagnostics, Mannheim, Germany) using TaqMan Universal PCR Master Mix and TaqMan Gene Expression Assays consisting of specific primers and FAM dye-labeled TaqMan minor groove binder probes (Applied Biosystems). The assay ID was Mm00516005_m1 for Hmox1 and Mm99999915_g1 for Gapdh. Amplification conditions were 50 °C for 2 min, 95 °C for 10 min, followed by 40 cycles at 95 °C for 15 s and 60 °C for 1 min. Crossing point values, equivalent to C_T, were determined automatically using the second derivative maximum analysis. Relative changes in gene expression were calculated by the comparative C_T method using the $2^{-\Delta\Delta C_T}$ equation with results normalized to Gapdh mRNA levels.

Western Blot Analyses. To prepare total cellular extracts, cells were washed with cold PBS, scraped from the plates, pelleted by centrifugation for 3 min at 1500 × g and 4 °C and lysed in lysis buffer (50 mM Tris, 150 mM NaCl, 1 mM EDTA, 1 mM NaF, 1 mM Na_3VO_4, 1 mM phenylmethylsulfonyl fluoride (PMSF), protease inhibitors Complete (Roche Diagnostics), 0.2% (m/v) sodium dodecyl sulfate (SDS), 1% (v/v) Nonidet-P40, 1% (v/v) Triton X-100, pH 7.4). After incubation on ice for 30 min, whole cell lysates were centrifuged for 10 min at 16 000 × g and 4 °C, and the supernatants were collected.

To prepare nuclear and cytosolic extracts, cells were collected from the plates as described above, and the cell pellets were resuspended in ice-cold buffer A (10 mM HEPES, pH 7.9, 10 mM KCl, 1.5 mM $MgCl_2$, 0.1% (v/v) Nonidet-P40, 0.5 mM dithiothreitol (DTT), protease inhibitors Complete). The cells were allowed to swell on ice for 10 min, centrifuged for 10 min at 12 000 × g and 4 °C, and the supernatants were collected as the cytosolic fraction. The pellets were vigorously resuspended in ice-cold buffer B (20 mM HEPES, pH 7.9, 420 mM NaCl, 1.5 mM $MgCl_2$, 0.2 mM EDTA, 25% (v/v) glycerol, 0.5 mM DTT, 0.5 mM PMSF) and incubated for 30 min on ice. The suspensions were centrifuged for 10 min at 12 000 × g and 4 °C, and the supernatants were collected as the nuclear fraction.

dx.doi.org/10.1021/jm3013344 | J. Med. Chem. 2013, 56, 856−866

Proteins in all samples were quantified using the Pierce BCA Protein Assay Kit (Thermo Scientific, Rockford, IL, USA). Aliquots containing an equal amount of protein were subjected to electrophoresis through 10% SDS−polyacrylamide gel, proteins were transferred to polyvinylidene difluoride membrane by electroblotting, and the membranes were probed with appropriate primary antibodies. Rabbit polyclonal heme oxygenase-1 (sc-10789), rabbit polyclonal Nrf2 (sc-722), goat polyclonal Keap1 (sc-15246), and goat polyclonal actin (sc-1616) antibodies were obtained from Santa Cruz Biotechnology (Santa Cruz, CA, USA). Rabbit polyclonal phospho-p44/42 MAPK (ERK1/2) (Thr202/Tyr204) (#9101), rabbit polyclonal p44/42 MAPK (ERK1/2) (#9102), rabbit polyclonal phospho-SAPK/JNK (Thr183/Tyr185) (#9251), rabbit polyclonal SAPK/JNK (#9252), rabbit monoclonal phospho-p38 MAPK (Thr180/Tyr182) (D3F9) XP (#4511), and rabbit monoclonal p38 MAPK (D13E1) XP (#8690) antibodies were obtained from Cell Signaling Technology (Danvers, MA, USA). Primary antibodies were visualized with rabbit anti-goat or goat anti-rabbit horseradish peroxidase-conjugated secondary antibodies using a chemiluminescent reaction. The relative band intensities were determined by densitometric analysis using ImageJ software (National Institutes of Health, Bethesda, MD, USA).

Flow Cytometric Detection of ROS. RAW264.7 cells were treated with 7-*O*-galloyltaxifolin or with 100 μM *tert*-butyl hydroperoxide (TBHP; positive control; Merck). After treatment, cells were centrifuged for 3 min at 110 × *g*, and the medium was exchanged for fresh serum-free medium. To detect intracellular ROS, cells were incubated with 10 μM 5-(and-6)-carboxy-2′,7′-dichlorodihydrofluorescein diacetate[17] (carboxy-H_2DCFDA; Invitrogen) for 15 min at 37 °C. After incubation, cells were scraped from the plate and immediately analyzed by flow cytometry on a Cytomics FC 500 (Beckman Coulter, Fullerton, CA, USA). Cells were excited with a 488-nm argon laser line and analyzed on FL1 channel (525 nm), counting 10 000 events per sample. The percentage of cells with increased ROS levels was calculated using MultiCycle AV software (Phoenix Flow Systems, San Diego, CA, USA).

Statistical analysis. Results were expressed as means ± standard deviation (SD). The differences in mean values were analyzed by Student *t*-tests. A *p* value of less than 0.05 was considered to be statistically significant.

■ ASSOCIATED CONTENT

Supporting Information

Preparation of compounds **5**−**7**, HPLC chromatograms and HRMS spectra of studied compounds **3** and **8**, ^{1}H and ^{13}C NMR data of compounds **2**, **3**, **5**, **7**, and **8**, MS fragmentation patterns of compounds **3** and **8** and of the oxidation product of compound **3**. This material is available free of charge via the Internet at http://pubs.acs.org.

■ AUTHOR INFORMATION

Corresponding Author

*Phone: +420 585632310. Fax: +420 585632302. E-mail: vrbambv@seznam.cz.

Author Contributions

All authors have given approval to the final version of the manuscript.

Notes

The authors declare no competing financial interest.

■ ACKNOWLEDGMENTS

We thank Dr Alexander Oulton for providing linguistic assistance. This work was supported by Grant P301/11/0767 from the Czech Science Foundation, by Grant CZ.1.05/2.1.00/01.0030 and Grant CZ.1.05/2.1.00/03.0058 from the Ministry of Education, Youth and Sports of the Czech Republic, and by Grant LF_2012_010 from Palacký University.

■ ABBREVIATIONS USED

3GQ, 3-*O*-galloylquercetin; 7GT, 7-*O*-galloyltaxifolin; APCI, atmospheric pressure chemical ionization; carboxy-H_2DCFDA, 5-(and-6)-carboxy-2′,7′-dichlorodihydrofluorescein diacetate; EGF, epidermal growth factor; ERK, extracellular signal-regulated kinase; ESI-QqTOF MS, electrospray ionization/quadrupole time-of-flight mass spectrometry; GA, gallic acid; *Gapdh*, glyceraldehyde-3-phosphate dehydrogenase gene; HEPES, 4-(2-hydroxyethyl)piperazine-1-ethanesulfonic acid; *Hmox1*, heme oxygenase-1 gene; HO-1, heme oxygenase-1; IQ, isoquercitrin; JNK, c-Jun N-terminal kinase; Keap1, Kelch-like ECH-associated protein 1; MAPK, mitogen-activated protein kinase; MTT, 3-(4,5-dimethylthiazol-2-yl)-2,5-diphenyltetrazolium bromide; NAC, *N*-acetyl-L-cysteine; Nrf2, nuclear factor erythroid 2-related factor 2; p38 MAPK, p38 mitogen-activated protein kinase; PD98059, 2-(2-amino-3-methoxyphenyl)-4*H*-1-benzopyran-4-one; PMSF, phenylmethylsulfonyl fluoride; QUE, quercetin; SB203580, 4-(4-fluorophenyl)-2-(4-methylsulfinylphenyl)-5-(4-pyridyl)-1*H*-imidazole; SP600125, 1,9-pyrazoloanthrone; TAX, taxifolin

■ REFERENCES

(1) Manach, C.; Scalbert, A.; Morand, C.; Remesy, C.; Jimenez, L. Polyphenols: Food sources and bioavailability. *Am. J. Clin. Nutr.* **2004**, *79*, 727−747.

(2) Santos, D. Y.; Salatino, M. L. Foliar flavonoids of *Annonaceae* from Brazil: Taxonomic significance. *Phytochemistry* **2000**, *55*, 567−573.

(3) Kim, Y.; Jang, D. S.; Park, S. H.; Yun, J.; Min, B. K.; Min, K. R.; Lee, H. K. Flavonol glycoside gallate and ferulate esters from *Persicaria lapathifolia* as inhibitors of superoxide production in human monocytes stimulated by unopsonized zymosan. *Planta Med.* **2000**, *66*, 72−74.

(4) Surh, Y. J.; Kundu, J. K.; Na, H. K. Nrf2 as a master redox switch in turning on the cellular signaling involved in the induction of cytoprotective genes by some chemopreventive phytochemicals. *Planta Med.* **2008**, *74*, 1526−1539.

(5) Acharya, A.; Das, I.; Chandhok, D.; Saha, T. Redox regulation in cancer: A double-edged sword with therapeutic potential. *Oxid. Med. Cell. Longevity* **2010**, *3*, 23−34.

(6) Li, W.; Khor, T. O.; Xu, C.; Shen, G.; Jeong, W. S.; Yu, S.; Kong, A. N. Activation of Nrf2-antioxidant signaling attenuates NFκB-inflammatory response and elicits apoptosis. *Biochem. Pharmacol.* **2008**, *76*, 1485−1489.

(7) Nguyen, T.; Nioi, P.; Pickett, C. B. The Nrf2-antioxidant response element signaling pathway and its activation by oxidative stress. *J. Biol. Chem.* **2009**, *284*, 13291−13295.

(8) Tanigawa, S.; Fujii, M.; Hou, D. X. Action of Nrf2 and Keap1 in ARE-mediated NQO1 expression by quercetin. *Free Radical Biol. Med.* **2007**, *42*, 1690−1703.

(9) Na, H. K.; Kim, E. H.; Jung, J. H.; Lee, H. H.; Hyun, J. W.; Surh, Y. J. (−)-Epigallocatechin gallate induces Nrf2-mediated antioxidant enzyme expression via activation of PI3K and ERK in human mammary epithelial cells. *Arch. Biochem. Biophys.* **2008**, *476*, 171−177.

(10) Wu, C. C.; Hsu, M. C.; Hsieh, C. W.; Lin, J. B.; Lai, P. H.; Wung, B. S. Upregulation of heme oxygenase-1 by epigallocatechin-3-gallate via the phosphatidylinositol 3-kinase/Akt and ERK pathways. *Life Sci.* **2006**, *78*, 2889−2897.

(11) Chen, C.; Yu, R.; Owuor, E. D.; Kong, A. N. Activation of antioxidant-response element (ARE), mitogen-activated protein kinases (MAPKs) and caspases by major green tea polyphenol components during cell survival and death. *Arch. Pharm. Res* **2000**, *23*, 605−612.

(12) Gazak, R.; Valentova, K.; Fuksova, K.; Marhol, P.; Kuzma, M.; Medina, M. A.; Oborna, I.; Ulrichova, J.; Kren, V. Synthesis and antiangiogenic activity of new silybin galloyl esters. *J. Med. Chem.* **2011**, *54*, 7397−7407.
(13) Russo, M.; Spagnuolo, C.; Tedesco, I.; Bilotto, S.; Russo, G. L. The flavonoid quercetin in disease prevention and therapy: Facts and fancies. *Biochem. Pharmacol.* **2012**, *83*, 6−15.
(14) Weidmann, A. E. Dihydroquercetin: More than just an impurity? *Eur. J. Pharmacol.* **2012**, *684*, 19−26.
(15) Chow, J. M.; Shen, S. C.; Huan, S. K.; Lin, H. Y.; Chen, Y. C. Quercetin, but not rutin and quercitrin, prevention of H_2O_2-induced apoptosis via anti-oxidant activity and heme oxygenase 1 gene expression in macrophages. *Biochem. Pharmacol.* **2005**, *69*, 1839−1851.
(16) Vrba, J.; Orolinova, E.; Ulrichova, J. Induction of heme oxygenase-1 by *Macleaya cordata* extract and its constituent sanguinarine in RAW264.7 cells. *Fitoterapia* **2012**, *83*, 329−335.
(17) Eruslanov, E.; Kusmartsev, S. Identification of ROS using oxidized DCFDA and flow-cytometry. *Methods Mol. Biol.* **2010**, *594*, 57−72.
(18) Loo, G. Redox-sensitive mechanisms of phytochemical-mediated inhibition of cancer cell proliferation (review). *J. Nutr. Biochem.* **2003**, *14*, 64−73.
(19) Boutros, T.; Chevet, E.; Metrakos, P. Mitogen-activated protein (MAP) kinase/MAP kinase phosphatase regulation: Roles in cell growth, death, and cancer. *Pharmacol. Rev.* **2008**, *60*, 261−310.
(20) Henklova, P.; Vrzal, R.; Papouskova, B.; Bednar, P.; Jancova, P.; Anzenbacherova, E.; Ulrichova, J.; Maurel, P.; Pavek, P.; Dvorak, Z. SB203580, a pharmacological inhibitor of p38 MAP kinase transduction pathway activates ERK and JNK MAP kinases in primary cultures of human hepatocytes. *Eur. J. Pharmacol.* **2008**, *593*, 16−23.
(21) Murakami, A.; Ashida, H.; Terao, J. Multitargeted cancer prevention by quercetin. *Cancer Lett.* **2008**, *269*, 315−325.
(22) Chosson, E.; Chaboud, A.; Chulia, A. J.; Raynaud, J. Dihydroflavonol glycosides from *Rhododendron ferrugineum*. *Phytochemistry* **1998**, *49*, 1431−1433.
(23) Manach, C.; Williamson, G.; Morand, C.; Scalbert, A.; Remesy, C. Bioavailability and bioefficacy of polyphenols in humans. I. Review of 97 bioavailability studies. *Am. J. Clin. Nutr.* **2005**, *81*, 230S−242S.
(24) Vacek, J.; Papouskova, B.; Kosina, P.; Vrba, J.; Kren, V.; Ulrichova, J. Biotransformation of flavonols and taxifolin in hepatocyte *in vitro* systems as determined by liquid chromatography with various stationary phases and electrospray ionization-quadrupole time-of-flight mass spectrometry. *J. Chromatogr. B* **2012**, *899*, 109−115.
(25) Gatto, M. T.; Falcocchio, S.; Grippa, E.; Mazzanti, G.; Battinelli, L.; Nicolosi, G.; Lambusta, D.; Saso, L. Antimicrobial and anti-lipase activity of quercetin and its C2-C16 3-O-acyl-esters. *Bioorg. Med. Chem.* **2002**, *10*, 269−272.
(26) Yeh, C. T.; Yen, G. C. Involvement of p38 MAPK and Nrf2 in phenolic acid-induced P-form phenol sulfotransferase expression in human hepatoma HepG2 cells. *Carcinogenesis* **2006**, *27*, 1008−1017.
(27) Yao, P.; Nussler, A.; Liu, L.; Hao, L.; Song, F.; Schirmeier, A.; Nussler, N. Quercetin protects human hepatocytes from ethanol-derived oxidative stress by inducing heme oxygenase-1 via the MAPK/Nrf2 pathways. *J. Hepatol.* **2007**, *47*, 253−261.
(28) Yeh, C. T.; Ching, L. C.; Yen, G. C. Inducing gene expression of cardiac antioxidant enzymes by dietary phenolic acids in rats. *J. Nutr. Biochem.* **2009**, *20*, 163−171.
(29) Naito, Y.; Takagi, T.; Yoshikawa, T. Heme oxygenase-1: a new therapeutic target for inflammatory bowel disease. *Aliment. Pharmacol. Ther.* **2004**, *20*, 177−184.
(30) Wu, M. L.; Ho, Y. C.; Lin, C. Y.; Yet, S. F. Heme oxygenase-1 in inflammation and cardiovascular disease. *Am. J. Cardiovasc. Dis* **2011**, *1*, 150−158.
(31) Maher, P.; Hanneken, A. Flavonoids protect retinal ganglion cells from oxidative stress-induced death. *Invest. Ophthalmol. Visual Sci.* **2005**, *46*, 4796−4803.
(32) Lukacin, R.; Wellmann, F.; Britsch, L.; Martens, S.; Matern, U. Flavonol synthase from *Citrus unshiu* is a bifunctional dioxygenase. *Phytochemistry* **2003**, *62*, 287−292.
(33) Rogozhin, V. V.; Peretolchin, D. V. Kinetic regulations of dihydroquercetin oxidation with horseradish peroxide. *Russ. J. Bioorg. Chem.* **2009**, *35*, 576−580.
(34) Vrba, J.; Kren, V.; Vacek, J.; Papouskova, B.; Ulrichova, J. Quercetin, quercetin glycosides and taxifolin differ in their ability to induce AhR activation and CYP1A1 expression in HepG2 cells. *Phytother. Res.* **2012**, *26*, 1746−1752.
(35) Weignerova, L.; Marhol, P.; Gerstorferova, D.; Kren, V. Preparatory production of quercetin-3-β-D-glucopyranoside using alkali-tolerant thermostable α-L-rhamnosidase from *Aspergillus terreus*. *Bioresour. Technol.* **2012**, *115*, 222−227.